Proceedings of the 35th European Safety and Reliability & the 33rd Society for Risk Analysis Europe Conference
Edited by Eirik Bjorheim Abrahamsen, Terje Aven, Frederic Bouder, Roger Flage, Marja Ylönen
 Published by Research Publishing, Singapore.
doi: 10.3850/978-981-94-3281-3_ESREL-SRA-E2025-P5944-cd

Stochastic risk assessment of railway masonry arch bridges in seismic prone areas in Portugal

Carlos Cabanzo
University of Minho, ISISE, ARISE, Department of Civil Engineering.E-mail: carlos.cabanzo@civil.uminho.pt

Rafael Amaral Torres
University of Minho, ISISE, ARISE, Department of Civil Engineering.E-mail: pg50702@alunos.uminho.pt

Hélder S. Sousa
University of Minho, ISISE, ARISE, Department of Civil Engineering.E-mail: sousa.hms@gmail.com

Mitsuyoshi Akiyama
Waseda University, Department of Civil and Environmental Engineering.E-mail: akiyama617@waseda.jp

Paulo B. Lourenço
University of Minho, ISISE, ARISE, Department of Civil Engineering.E-mail: pbl@civil.uminho.pt

José C. Matos
University of Minho, ISISE, ARISE, Department of Civil Engineering.E-mail: jmatos@civil.uminho.pt

Risk-based methodologies for analyzing transportation assets have been employed to ensure good performance and long-term safety. Failure of transportation structures leads to major economic consequences, often due to the uncertainties associated with these structures and the effects of unexpected extreme events. Generally, risk is described by hazard intensity, vulnerability, and consequences related to the probability of a given hazard to occur, the susceptibility of a system to be affected by said hazard, and the quantification of the effects, respectively. In Portugal, large masonry arch bridges (MABs) were built during the railway expansion to improve the national network. These structures are expected to continue operating as a crucial part of the railway network without elevated maintenance costs. The present research presents a risk analysis of two of the largest masonry arch bridges built during this period. A risk index is computed based on the combination of code-based hazard curves, seismic fragility curves, and direct consequences. The risk assessment considers material uncertainties, damage states, and peak ground acceleration as the seismic intensity measure. The resulting risk curves provide useful information for prioritizing assets' interventions and taking preventive actions to maintain the desired performance of the railway system.

Keywords: Seismic vulnerability curves, railway networks, parameter uncertainty, asset management.

1. Introduction

Railway systems are a key part of the development of many countries, and asset failures can have significant consequences. Asset management is essential to maintain performance, with risk-based approaches prioritizing interventions based on the probability and impact of failure modes under expected hazards (Papathanasiou and Adey, 2021). Masonry arch bridges (MABs) represent a significant part of the stock in many European railway networks, contributing to the economic growth (Sarhosis et al., 2016). Despite being designed for lower loads than the current ones, MABs remain in service with minimal maintenance. Performance assessment of MABs is critical for transportation authorities, especially since larger multi-span MABs are vulnerable to seismic actions (Zampieri et al., 2021).

Research on multi-span MABs has focused on their mechanical and modal properties for numerical model calibration (Pantò et al., 2024; Shabani and Kioumarsi, 2023; Zampieri et al., 2021;

Neto, 2015). Stochastic analyses have quantified the effects of uncertainties in mechanical properties through reliability (Gönen and Soyöz, 2022), fragility (Cabanzo et al., 2025; Barbieri, 2019), and vulnerability analyses (Barbieri, 2019; Cucuzza et al., 2024). However, these approaches might present limitations when prioritizing assets since often they do not account for the consequences of failure (Papathanasiou and Adey, 2021).

Risk-based methodologies offer insights into both the probability of failure and the consequences within the network. Some studies have assessed seismic risk for bridge stock (Burton and Vitor Silva, 2014; Saler et al., 2021; Li and Formisano, 2023), but the inclusion of uncertainty in risk assessments of multi-span MABs has been limited.

The present research analyzes the seismic performance of three multi-span MABs built during the railway expansion in the 1930s. The resulting stochastic risk curves were derived by considering different damage states and employing code-based response spectra and hazard curves, enabling the comparison and prioritization of interventions within the transportation network. The resulting vulnerability curves are derived using peak ground acceleration (PGA) as the intensity measure (IM) and spectral displacement as the conditioning for the failure of each damage state. Moreover, the direct consequences were estimated based on the cost of rebuilding with an uncertainty parameter to allow a more accurate estimation of the costs of each of the damaged states.

2. Multi-span MABs

In Portugal, masonry arch bridges (MABs) represent around 30% of the total stock in the railway network, where 10% account for large bridges, most of which were built between 1850 and 1950 period of significant railway expansion (Silva, 2022). During this period, around 1912, the former Portuguese railway administration identified large degradation patterns in the larger steel bridges, which led to a nationwide project to replace them for MABs. However, their construction would be delayed until the 1930s due to several reasons, including the First World War (Costa, 1934). Figure 1 shows the Quinta Nova bridge in southern Portugal as an example of masonry structures that replaced a former steel structure during the first half of the 20th century.

Fig. 1. Composition of the actual Quinta Nova bridge in September 2023 and its construction process during June 1933, showcasing the original metallic structure in the background. Adapted from (Costa, 1934).

2.1. *Case studies*

Southern Portugal is associated with high seismicity; within this region, in the 1930s, around 26 steel bridges were replaced by MABs; two of the larger structures include the Mouratos and the Quinta Nova bridges (see Figure 2) (Costa, 1934). These bridges are part of the second most important railway line of the country, known as the "*Linha do Sul*" and are used to transport goods between the port in the capital city of Lisbon and the southern region of Algarve. During the latter part of the railway expansion in 1948, the Côa bridge, one of the largest MAB built within the scope of the project, finished construction as part of the "*Beira Alta*" railway line in Northern Portugal (Costa, 1948). These bridges were selected as case studies since they provide a good combination of scale and seismic exposure (see Figure 2).

2.2. *Numerical modeling*

Three-dimensional finite element models employing the macro-modeling approach were developed for each case study to derive the fragility curves. The FEM was implemented through DIANA FEA

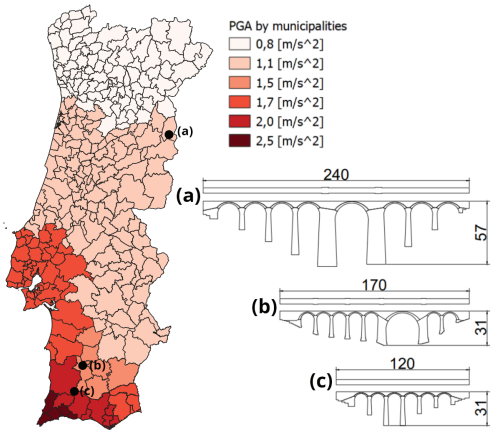

Fig. 2. General geometry of the case studies (a) Côa, (b) Quinta Nova, and (c) Mouratos. Localization in the seismic hazard map with the different values of max PGA per municipality. Based on (CEN, 2004).

software (FEA, 2023), employing 3D quadrilateral elements. The mechanical properties of the materials,*e.g.*, elasticity modulus, were retrieved and calibrated using the available information of the dynamic identification tests considering the first three out-of-plane modal frequencies (see Figure 3) (Cabanzo et al., 2025; Neto, 2015). There was no available modal information on the Mouratos bridge; however, the resulting calibrated elasticity moduli of the Quinta Nova bridge were used since both bridges were designed and constructed in parallel (Costa, 1934). A modal pushover analysis was performed to determine the seismic capacity of the bridges employing a mode-dependent equivalent lateral force. The numerical solution of the nonlinear equations was obtained using the Modified Newton-Raphson iterative method with a convergence norm based on energy with a tolerance equal to 0.001 (FEA, 2023).

2.3. *Damage and performance limit states*

Damage states (DS) describe the physical condition of a structure limited by the performance limit states (PL). For this research, the PLs will be defined according to the return periods of 225, 475, and 2475 years, given in the Eurocode (CEN, 2004). In literature, equivalent definitions

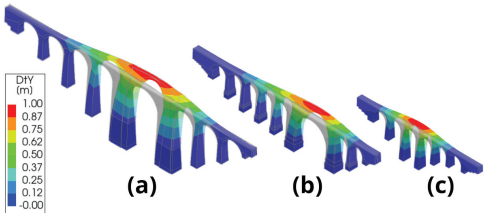

Fig. 3. Modal shapes and frequencies of the first mode: (a) Côa f_1 : $1.14Hz$, (b) Quinta Nova f_1 : $3.03Hz$, and (c) Mouratos f_1 : $3.54Hz$.

of damage states have been successfully applied to the seismic fragility of multi-span MABs (Shimpi et al., 2021; Shabani and Kioumarsi, 2023; Gönen and Soyöz, 2022). Moreover, an equivalent bilinear idealization of the pushover curve according to the Italian guidelines was employed (De Luca et al., 2013) (see Figure 4 for a visual representation). The following PL were considered:

- *PL1*-Damage limitation is associated with a predominantly elastic response. Limit between *DS1* (Elastic behavior) and the start of the plastic behavior. *DS2* (No collapse);
- *PL2*-Significant damage represents the limit where the structure maintains its integrity. Assumed as the point of a 50% reduction of the stiffness of the pushover curve, limiting *DS2* (No collapse) and *DS3* (Near collapse);
- *PL3*-Near collapse is often associated with the collapse of the structure. Represented by the endpoint in the pushover curve and indicates the start of *DS4*(Collapse).

3. Risk assessment

3.1. *Seismic hazard*

The seismic hazard was considered as seismic action type 1 presented in the Eurocode 8 (CEN, 2004). The employed demand spectrum is associated with a given return period, T, and a given peak ground acceleration (PGA) based on the Portuguese seismic zones (Sz). Table 1 presents the information related to the location of the bridges and their associated seismic zones. Figure 5 presents the hazard curves presenting the probability of exceedance of a seismic action with a given intensity.

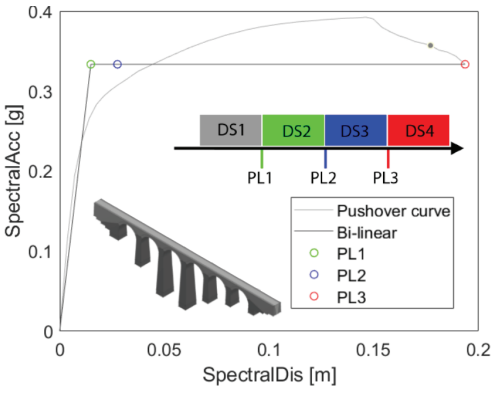

Fig. 4. Performance limit states and bi-linear approximation of the pushover curve considering a 15% reduction of the maximum base and 60% of the initial stiffness for the Mouratos bridge

3.2. *Fragility analysis*

Parameter uncertainty was included according to the JCSS probabilistic model code (Vrouwenvelder, 1997) by the introduction of independent lognormal variables associated with the elasticity modulus and the compressive strength with mean value 1 and coefficient of variation of 25% and 20%, respectively. Moreover, to address the computational cost associated with the stochastic analysis, a support vector machine for the classification surrogate model was introduced through UQLab (Marelli and Sudret, 2014), including a sequential sampling approach (Vořechovský, 2022). The classification of failure or success is achieved by comparing the demand spectrum with the bi-linear pushover curve for each PLs. Then, importance sampling was employed to obtain the failure probability of each PL (Tabandeh et al., 2022). A detailed framework for the derivation of seismic fragility curves is presented in Cabanzo et al. (2025), where the Quinta Nova bridge is used as a case study. Figure 6 presents the resulting pushover curves considering the uncertainties for the Mouratos bridge.

Table 1. Localization of the bridges with their corresponding seismic zones of type 1 actions.

Bridge	Municipality	Seismic zone	Reference PGA $[m/s^2]$
Côa	Almeida	1.6	0.35
Quinta Nova	Ourique	1.3	1.50
Mouratos	Odemira	1.2	2.00

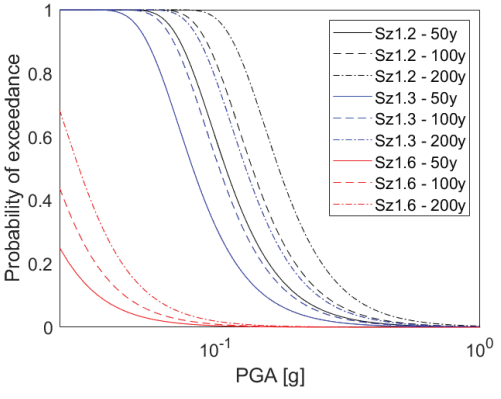

Fig. 5. Hazard curves of the seismic zones of each case study: (Sz 1.3) Côa, (Sz 1.6) Quinta Nova and (Sz 1.2) Mouratos for different time spans, 50, 100, and 200 years

The lognormal fragility curves are obtained by correlating the maximum PGA of the demand spectrum as the intensity measure, with the exceedance probability of surpassing each performance limit state. Figure 7 presents the damage curves with the probability of the asset being in a given DS for a given seismic intensity in terms of PGA. The Côa bridge presents a higher probability of exceedance of each PL for lower values of PGA, which correlates with the lower values of its

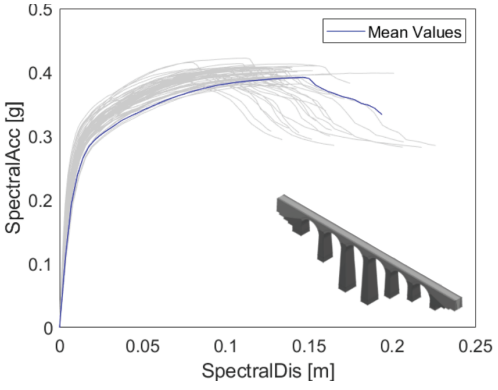

Fig. 6. Pushover curves obtained for the Mouratos bridge after including parameter uncertainties.

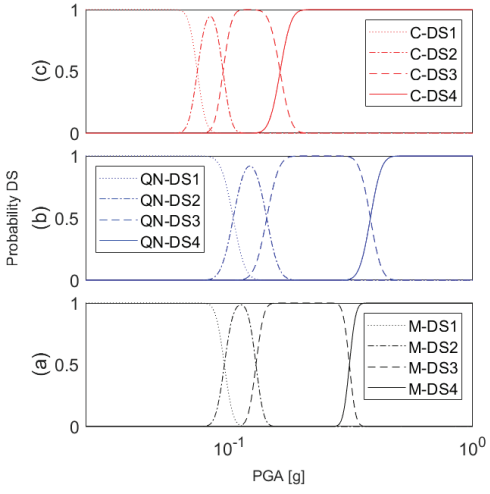

Fig. 7. Seismic damage curves considering the *DS1*-Elastic behavior, *DS2*-No collapse, *DS3*-Near collapse, and *DS4*-Collapse for each bridge: (a) Côa, (b) Quinta Nova, and (c) Mouratos.

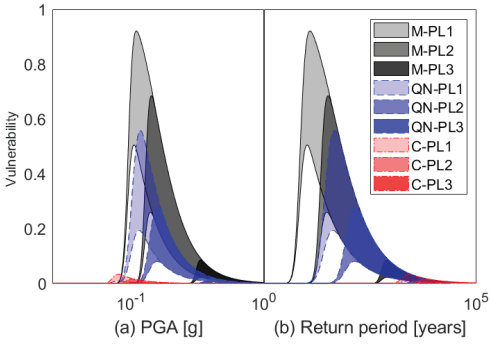

Fig. 8. Seismic Vulnerability curves considering the *PL1*-Damage limitation, *PL2*-Significant damage, and *PL3*-Near collapse for time spans between 50 and 200 years. Bridges: C-Côa, QN-Quinta Nova, and M-Mouratos.

mechanical parameters. Moreover, the Mouratos and Quinta Nova bridges present similar fragility curves, which can be explained by both employing similar values for their mechanical properties.

3.3. *Vulnerability assessment*

Vulnerability can be defined as the cumulative failure probability of a given performance limit state, *i.e.*, fragility curve, under a given IM (Li and Formisano, 2023). In this research, the seismic hazard curves are combined with the fragility curve of each PLs for each case study to estimate the seismic vulnerability. Figure 8 presents the seismic vulnerability curves for each of the three assets.

From the vulnerability curves, it can be concluded that when comparing the seismic intensity, the Côa bridge presents the highest vulnerability for lower values of intensity. However, when comparing the vulnerability curves in terms of return periods, it is observed that the range of intensities is equal to high return periods due to the low seismicity of the municipality where it is located. Moreover, although the Mouratos and Quinta Nova bridges present similar values of fragility, the former is located in a municipality with higher exposure, *i.e.*, higher probability of exceedance of a given seismic intensity, thus yielding a higher vulnerability. Table 2 presents an adaptation of the categorization based on exceedance probability employed by (Saler et al., 2021) for the prioritization of assets based on their seismic vulnerability.

Table 3 presents the results of the exceedance probability for each case study. From the results, it can be concluded that they have a good seismic capacity since they present low values of probability of exceedance for the PL3, *i.e.*, collapse. For the Quinta Nova and Mouratos bridges, the failure probability is caped at 10%, which is the exceedance probability in the code for the reference action, meaning that their fragility for that given PL is 1. Similarly, in Figure 8b, the vulnerability aligns with the hazard curve after each PL reaches a probability of exceedance of 1.

Table 2. Vulnerability classification based on the occurrence probability.

Vulnerability level	Probability [%]
1	≤0.01%
2	[0.01%-0.10%]
3	[0.10%-0.50%]
4	[0.50%-10.00%]
5	≥10.00%

Adapted from: Saler et al. (2021).

Table 3. Classification of the asset based on the probability of exceedance of each PL for an action with a return period of 475 years in a time span of 50 years.

Bridge	Probability of exceedance			Lowest DS	Vul index*
	PL1	PL2	PL3		
Côa	3e-31	6e-55	5e-78	DS1	1
Quinta Nova	0.10	0.08	8e-30	DS2	4
Mouratos	0.10	0.10	8e-21	DS3	5

Note:: *Vulnerability index ranges from 1-low to 5-high vulnerability.

3.4. *Direct consequences*

An analysis of the consequences of surpassing a given PL might help prioritize interventions within a transportation network. These consequences can be divided into direct and indirect consequences. The former relates to the costs of rebuilding or reparation, depending on the given PL. Meanwhile, the indirect consequences can be related to costs resulting from delays in travel times, casualties, unavailability of the network, and operational costs, among others. Moreover, when accounting for the costs associated with a given consequence, it is important to consider the change in time of the currency that is being employed (Decò and Frangopol, 2013).

Figure 9 presents the direct consequences DC associated with the cost of rebuilding C_{Reb} per area and the dimensions of the bridge, W and L for the width and length respectively. Moreover, it considers the adjustment rate r of Portugal and the uncertainty factor E_{Reb}, which follows a log-normal distribution with mean one and coefficient of variation of 20%, for the next 200 years based on the Eq. (1) (Decò and Frangopol, 2013). The C_{Reb} and r were employed in accordance with the results from previous cost analyses of different MABs in Portugal (Almeida, 2013; Silva, 2020).

$$DC = E_{Reb} \cdot C_{Reb} \cdot W \cdot L \cdot (1+r)^t \quad (1)$$

3.5. *Seismic risk curves*

The primary objective of the risk assessment is to support the decision-making process in asset management by identifying the most critical infrastructure or components where actions to mitigate or avoid the risks associated with a seismic scenario are required. However, performing such analyses requires a high complexity and quantity of information, thus making it challenging to apply to a large stock of assets (Papathanasiou and Adey, 2021). Therefore, it is necessary to develop a risk-based methodology that allows the prioritization of assets and optimizes the available resources.

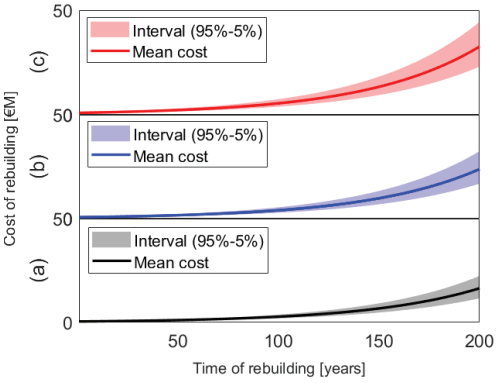

Fig. 9. Direct consequences associated to the cost of rebuilding based on Eq. (1) considering the adjustment rate and the uncertainty factor for the different case studies: (a) Mouratos, (b) Quinta Nova, and (c) Côa

Figure 10 presents the seismic curves for each asset obtained by combining the hazard curves for a time span of 50 years (see Figure 5) with the probability of an asset being in a given DS (see Figure 7) and the associated costs of consequences (see Figure 9). For computing the cost of each DS, an approximation based on the residual capacity of the asset was employed, meaning that for a *DS4* and *DS1*, the costs will be equal to 100% and 0% of the costs of rebuilding, since the associated residual capacity is 0% and 100%, respectively. For the *DS2* and *DS3*, the residual capacity was computed as a relation between the maximum displacement of the pushover curve and the displacement of *PL1* and *PL2*.

4. Conclusions

The proposed research is significant to the railway management authorities because it allows the direct comparison of risk levels of different

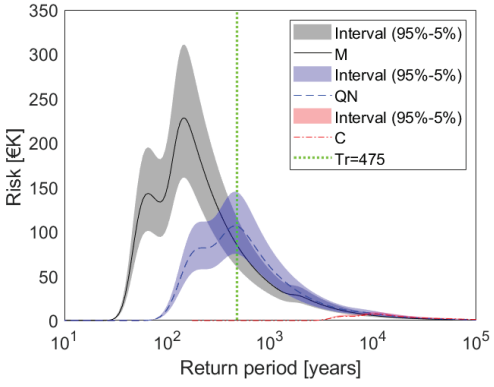

Fig. 10. Seismic risk curve in terms of the return period of a seismic action type in a time span of 50 years, considering the uncertainty of the consequences for each bridge: C-Côa, QN-Quinta Nova, and M-Mouratos.

multi-span MABs within the railway network, thus allowing a better allocation of the available resources.

The findings show that fragility might not be enough to correctly prioritize assets in the network. Exposure to the hazard and the consequences associated with each limit state must also be included. The Côa, while being the largest structure and the most susceptible to out-of-plane effects, is located in a region in Portugal with low seismic hazard, thus resulting in the lowest priority. On the contrary, the Mouratos bridge, while being the smallest, is located in a region with high seismic risk, thus yielding the highest priority.

The present research has some limitations that may be addressed in future works. Seismic fragility curves were obtained for a seismic action type 1 based on the seismic zone of the Eurocode. However, in northern Portugal, some regions might experience a more critical effect of seismic action type 2. Moreover, a seismic map obtained through probabilistic seismic hazard assessment might be more accurate.

Only direct consequences associated with the cost of rebuilding were considered; however, indirect consequences are relevant and might affect the priority of interventions, especially for bridges, part of a key branch of the railway network.

Acknowledgement

This work is financed by national funds through FCT - Foundation for Science and Technology, under grant agreement 2022.09751.BD attributed to the 1st author. This work was partly financed by FCT / MCTES through national funds (PIDDAC) under the R&D Unit Institute for Sustainability and Innovation in Structural Engineering (ISISE), under reference UIDB / 04029/2020 (doi.org/10.54499/UIDB/04029/2020), and under the Associate Laboratory Advanced Production and Intelligent Systems ARISE under reference LA/P/0112/2020.

References

Almeida, J. (2013). *Sistema de gestão de pontes com base em custos de ciclo de vida*. PhD thesis, Universidade do Porto, Porto, Portugal.

Barbieri, D. M. (2019, February). Two methodological approaches to assess the seismic vulnerability of masonry bridges. *Journal of Traffic and Transportation Engineering (English Edition) 6*(1), 49–64.

Burton, C. and Vitor Silva (2014). Integrated Risk Modeling Within The Global Earthquake Model (Gem): Test Case Application For Portugal. Publisher: Unpublished.

Cabanzo, C., N. Mendes, M. Akiyama, P. B. Lourenço, and J. C. Matos (2025, February). Probabilistic framework for seismic performance assessment of a multi-span masonry arch bridge employing surrogate modeling techniques. *Engineering Structures 325*, 119399.

CEN (2004). Eurocode 8: Design of Structures for Earthquake Resistance. Part 1: General Rules, Seismic Actions and Rules for Buildings.

Costa, L. d. M. e. (1934, January). Caminhos de Ferro Nacionais. *Gazeta dos Caminhos de Ferro Ano 46*(1125), 547–550.

Costa, L. d. M. e. (1948, April). Linhas Portuguesas. *Gazeta dos Caminhos de Ferro Ano 60*(1448), 282.

Cucuzza, R., A. Aloisio, R. Di Bari, and M. Domaneschi (2024, March). Vulnerability assessment and lifecycle analysis of an existing masonry arch bridge. *Engineering Structures 302*, 117422.

De Luca, F., D. Vamvatsikos, and I. Iervolino (2013). Improving Static Pushover Analysis by Optimal Bilinear Fitting of Capacity Curves. In M. Papadrakakis, M. Fragiadakis, and V. Plevris (Eds.), *Computational Methods in Earthquake Engineering*, Volume 30, pp. 273–295. Dordrecht: Springer Netherlands. Series Title: Computational Methods in Applied Sciences.

Decò, A. and D. M. Frangopol (2013, February). Life-Cycle Risk Assessment of Spatially Distributed Ag-

ing Bridges under Seismic and Traffic Hazards. *Earthquake Spectra 29*(1), 127–153.

FEA, D. (2023). DIANA Finite Element Analysis (FEA) Software.

Gönen, S. and S. Soyöz (2022, December). Reliability-based seismic performance of masonry arch bridges. *Structure and Infrastructure Engineering 18*(12), 1658–1673.

Li, S.-Q. and A. Formisano (2023, June). Statistical model analysis of typical bridges considering the actual seismic damage observation database. *Archives of Civil and Mechanical Engineering 23*(3), 178.

Marelli, S. and B. Sudret (2014, June). UQLab: A Framework for Uncertainty Quantification in Matlab. In *Vulnerability, Uncertainty, and Risk*, Liverpool, UK, pp. 2554–2563. American Society of Civil Engineers.

Neto, J. A. D. (2015). *Calibração de modelos dinâmicos de pontes ferroviárias em arco de alvenaria de pedra*. Master of Science (MS), University of Porto, Porto, Portugal.

Pantò, B., J. Ortega, S. Grosman, D. Oliveira, P. Lourenço, L. Macorini, and B. Izzuddin (2024, August). Advanced calibration of a 3D masonry arch bridge model using non-destructive testing and numerical optimisation. *Construction and Building Materials 438*, 137131.

Papathanasiou, N. and B. T. Adey (2021, June). Making comparable risk estimates for railway assets of different types. *Infrastructure Asset Management 8*(2), 53–74.

Saler, E., V. Pernechele, G. Tecchio, and F. Da Porto (2021). APPLICATION TO AN URBAN BRIDGE STOCK OF A PRIORITIZATION PROCEDURE BASED ON SEISMIC ASSESSMENT COMPARED WITH THE NOVEL ITALIAN GUIDELINES. Athens, Greece, pp. 3484–3498.

Sarhosis, V., S. De Santis, and G. De Felice (2016, November). A review of experimental investigations and assessment methods for masonry arch bridges. *Structure and Infrastructure Engineering 12*(11), 1439–1464.

Shabani, A. and M. Kioumarsi (2023, October). Seismic assessment and strengthening of a historical masonry bridge considering soil-structure interaction. *Engineering Structures 293*, 116589.

Shimpi, V., M. V. R. Sivasubramanian, S. B. Singh, and D. K. Periyasamy (2021, June). Seismic vulnerability assessment and fragility curves for a multistorey gallery arch bridge. *SN Applied Sciences 3*(6), 662.

Silva, C. (2020). Sistema de gestão de obras de arte rodoviárias baseado na análise de custo de ciclo de vida. Master's thesis, Universidade do Porto, Porto, Portugal.

Silva, R. F. P. d. (2022). *Advanced non-linear numerical simulation tools for in-service and retrofitting assessment of stone masonry railway arch bridges – experimental calibration and validation*. Doctoral thesis, University of Porto, Porto, Portugal.

Tabandeh, A., G. Jia, and P. Gardoni (2022, July). A review and assessment of importance sampling methods for reliability analysis. *Structural Safety 97*, 102216.

Vořechovský, M. (2022, November). Reliability analysis of discrete-state performance functions via adaptive sequential sampling with detection of failure surfaces. *Computer Methods in Applied Mechanics and Engineering 401*, 115606.

Vrouwenvelder, T. (1997, January). The JCSS probabilistic model code. *Structural Safety 19*(3), 245–251.

Zampieri, P., C. D. Tetougueni, and C. Pellegrino (2021, December). Nonlinear seismic analysis of masonry bridges under multiple geometric and material considerations: Application to an existing seven-span arch bridge. *Structures 34*, 78–94.